

CHROM. 20 669

## CROSS-AXIS SYNCHRONOUS FLOW-THROUGH COIL PLANET CENTRIFUGE FOR LARGE-SCALE PREPARATIVE COUNTER-CURRENT CHROMATOGRAPHY

### I. APPARATUS AND STUDIES ON STATIONARY PHASE RETENTION IN SHORT COILS

YOICHIRO ITO\* and TIAN-YOU ZHANG\*

*Laboratory of Technical Development, National Heart, Lung, and Blood Institute, Bethesda, MD 20892 (U.S.A.)*

(First received March 14th, 1988; revised manuscript received May 26th, 1988)

---

#### SUMMARY

Using a new cross-axis synchronous flow-through coil planet centrifuge with a 20-cm revolutionary radius, the retention of the stationary phase for nine solvent systems was studied with short coils mounted at two different locations on three holders with 5-, 15- and 25-cm hub diameters. Coils mounted 10 cm to the left of the center of a holder produced a much improved retention of most of the solvent systems compared with the same coils mounted at the center of the holder. In the lateral coil position the retention was found to be affected by the direction of the planetary motion and the head-tail elution mode. This phenomenon may be attributed to the effect of the lateral force field acting asymmetrically between the upper and lower halves of the coil.

---

#### INTRODUCTION

Recently, a cross-axis synchronous flow-through coil planet centrifuge (X-axis CPC) has been developed in our laboratory for performing preparative counter-current chromatography (CCC). The system utilizes a novel mode of planetary motion to achieve highly efficient chromatographic separations of solutes on the preparative scale<sup>1,2</sup>. The centrifugal force field generated by this planetary motion provides efficient three-dimensional mixing of two solvent phases in a coiled column to nearly double the partition efficiency obtained by existing high-speed CCC systems<sup>3</sup>. The capability of the X-axis CPC has been demonstrated by preparative-scale separations of dinitrophenyl (DNP) amino acids and dipeptides by a prototype apparatus with a 10-cm revolutionary radius<sup>2</sup>. More recent studies have indicated that the system can be applied efficiently to form separations with a long multilayer coil<sup>4</sup>.

---

\* Permanent address: Beijing Institute of New Technology Application, Beijing, China.

In this paper we describe a further development of the X-axis CPC obtained by increasing both the revolutionary radius and column holder dimensions. A new large prototype with a 20-cm revolutionary radius has been tested with respect to stationary phase retention and partition efficiency using standard sets of two-phase solvent systems to compare the performance with those of existing high-speed CCC systems. The use of a large revolutionary radius and a proper choice of column orientation on the holder have considerably improved the retention of the stationary phase, especially for hydrophilic solvent systems, which are extremely useful for separating peptides and other polar compounds. Studies on the partition efficiency and preparative capability of the apparatus are described in Part II.

#### APPARATUS

The principle and basic design of the X-axis CPC have been described previously<sup>1</sup>. The synchronous planetary motion of the apparatus is illustrated schematically in Fig. 1, where the coil holder disc with the bundle of flow tubes is drawn in successive positions as it revolves around the central axis of the centrifuge. The disc revolves around the central axis of the centrifuge and simultaneously rotates about its own axis at the same angular velocity in the indicated directions. In doing so, the holder disc constantly maintains its axis in a tangential orientation to a path formed by revolution with a fixed distance,  $R$ , from the centrifuge axis. Consequently, the axes of revolution and rotation in the planetary motion form a cross to each other, hence the name of the instrument.

The above synchronous planetary motion bears two important functions for performing CCC. First, the synchronous rotation of the holder disc steadily unwinds the twist of the tubing caused by the revolution, thus permitting continuous elution of the mobile phase through the rotating column without the use of a rotary seal device, which would cause various complications such as leakage, contamination, etc. The

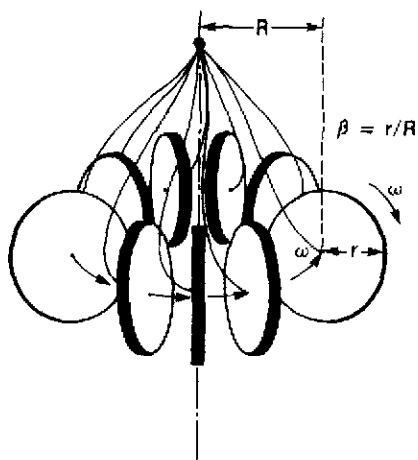


Fig. 1. Successive positions of coil holder in cross-axis synchronous flow-through coil planet centrifuge. Because of the synchronous planetary motion of the holder, the bundle of flow tubes becomes free of twisting.

planetary motion further generates a unique pattern of the centrifugal force field which permits more efficient chromatographic separations of solutes in a multilayer coil at a high flow-rate, as previously described<sup>1,2</sup>.

Fig. 2A is a photograph of the second prototype X-axis CPC with a 20-cm revolutionary radius used in these studies. The rotary frame of the apparatus consists of a pair of butterfly-shaped aluminium side-plates rigidly bridged together with upper and lower aluminium plates and several additional links to hold a column holder and a counterweight holder horizontally in symmetrical positions at a distance of 20 cm from the central axis of the centrifuge. The rotary frame is driven by a motor (Electro-Craft, Hopkins, MN, U.S.A.) via a pair of toothed pulleys, one mounted on

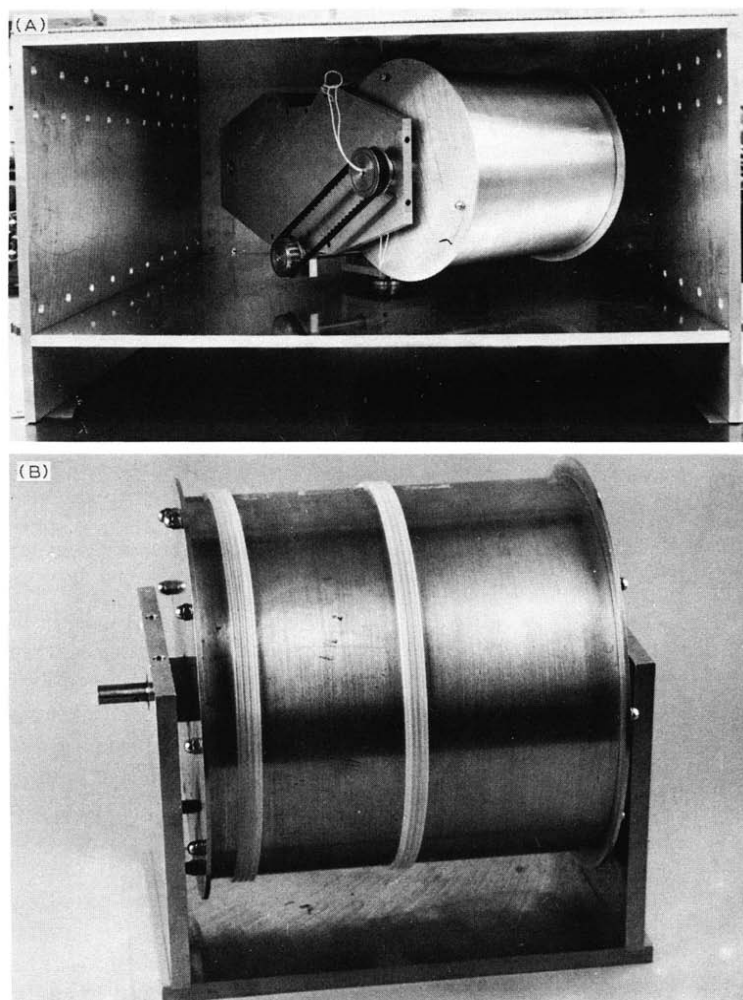


Fig. 2. (A) The cross-axis synchronous flow-through coil planet centrifuge with a 20-cm revolutionary radius. The apparatus holds a 25-cm diameter coil holder. (B) Central ( $l = 0$  cm) and lateral ( $l = -10$  cm) coil positions on the 25-cm diameter holder which is held on the stand.

the motor shaft and the other on the central shaft of the rotary frame, through a toothed belt at the bottom of the centrifuge. In order to support the heavy weight of the rotary frame (*ca.* 32 kg), a thrust bearing (not shown in the photograph) is embedded at the bottom plate of the centrifuge around the central shaft.

Synchronous planetary motion of the holders is introduced by means of coupling a set of three miter gears ( $45^\circ$ ), all identical in shape. One miter gear, called the stationary sun gear (plastic), is mounted rigidly on the bottom plate coaxially around the central shaft of the rotary frame, while other two planetary miter gears (steel) are positioned symmetrically over the sun gear. Each planetary gear is equipped with a countershaft which extends radially toward the periphery through a ball-bearing, embedded in the lower portion of the side-plate, to hold a toothed pulley securely on the distal end. The above gear arrangement produces a synchronous rotation of each countershaft on the revolving rotary frame. This motion is further conveyed to the respective holder by coupling the toothed pulley on the countershaft to the identical pulley mounted at one end of the holder shaft with a toothed belt. Consequently, both the column holder and counterweight holder undergo the desired synchronous planetary motion, *i.e.*, rotation around its own axis and revolution around the central axis of the centrifuge at the same angular velocity, as illustrated schematically in Fig. 1.

Flow tubes from the holder are first led through the center hole of the holder shaft and then, making a loop, passed through a guide ring attached to the side-plate to enter the side hole of the central shaft of the rotary frame where they exit the centrifuge through a stationary guide pipe projecting down from the top plate of the centrifuge. Near the exit hole, each flow tube is firmly held by a clamp equipped with a silicone-rubber pad. These flow tubes are lubricated with grease and protected by a piece of Tygon tubing to prevent direct contact with metal parts. With proper care, the flow tubes can maintain their function for many months of operation.

The revolutional speed of the apparatus can be regulated in a range between 0 and 500 rpm in either direction at high stability by a speed control unit (Electro-Craft). A plastic baffle placed close to the rotary frame around the periphery of the centrifuge case (not shown) reduced windage, resulting in a reduction of the torque by over 30% at the maximum speed of 500 rpm.

In order to apply various types of column holders in the same apparatus, both the column holder and counterweight holder are designed to be easily removable from the rotary frame simply by loosening a pair of screws on each bearing block. This design also facilitates mounting the coiled column on the holder and determining a proper counterweight mass to be applied for balancing the centrifuge system.

Two sets of column holders were fabricated. The first set consists of long spool-shaped holders (measuring 25 cm between the flanges) with different hub diameters ranging from 5 to 25 cm (the largest holder is shown in Fig. 2). Each holder is paired with a proper counterweight mass to be mounted on the counterweight holder. These column holders were used to measure stationary phase retention and partition efficiency in short coils mounted at two different locations on the holder, *i.e.*, at the center and at 10 cm to the left of the center (Fig. 2B). The second set consists of a pair of identical spool-shaped holders each measuring 5 cm between the flanges and 15 cm in hub diameter. These holders are used exclusively for mounting long multilayer coils suitable for large-scale preparative separations. They are mounted symmetrically on both sides of the rotary frame to effect perfect balancing of the centrifuge system

without the use of a counterweight. Two columns can be connected in series with a transfer tube or each can be used separately in tandem. Further details for the column design and preparation of the multilayer coils are described in Part II.

## EXPERIMENTAL

### *Reagents*

Two-phase solvent systems were prepared from *n*-hexane, ethyl acetate, chloroform, *n*-butanol, *sec.*-butanol and methanol (glass-distilled chromatographic grade, Burdick and Jackson Labs., Muskegon, MI, U.S.A.), acetic acid (reagent grade, J. T. Baker, Phillipsburg, NJ, U.S.A.) and distilled water.

### *Preparation of two-phase solvent systems*

The following nine volatile two-phase solvent systems were prepared: *n*-hexane-water, *n*-hexane-methanol, ethyl acetate-water, ethyl acetate-acetic acid water (4:1:4 by volume), chloroform-water, chloroform-acetic acid-water (2:2:1), *n*-butanol-water, *n*-butanol-acetic acid water (4:1:5) and *sec.*-butanol-water. Each solvent mixture was thoroughly equilibrated in a separatory funnel at room temperature by repeated shaking and degassing (by opening the stopcock), and separated before use.

### *Preparation of coiled columns*

These studies were performed with short coils of 2-3 m  $\times$  2.6 mm I.D. PTFE tubing (Zeus Industrial Products, Raritan, NJ, U.S.A.) wound coaxially around the holders of 5-, 15- and 25-cm hub diameters. For each holder, the coil was mounted at two different locations, either at the center of the holder ( $l = 0$  cm) or 10 cm to the left of the center of the holder ( $l = -10$  cm) (Fig. 2B). Although right-handed coils were mainly used, the left-handed coil was also tested at  $l = -10$  cm on the 25-cm diameter holder. These columns were firmly held on the holder with several pieces of fiber-glass reinforced adhesive tape.

Each end of the coil was directly connected to a 1 m  $\times$  0.85 mm I.D. flow tube without the use of a bulky commercial flanged connector, which would distort the helical configuration near the junction. The connection was made by inserting a series of smaller diameter tubing into one another, resembling concentric circles from the end, until the smallest I.D. of 0.85 mm emerges from the center. This tubing was PTFE with sizes 2.1 mm I.D. and 2.8 mm O.D. and also 1.3 mm I.D. and 2.1 mm O.D.

### *Measurement of stationary phase retention*

Experiments were performed according to a previously described procedure<sup>2</sup>. For each coil, retention was measured for the nine two-phase solvent systems. For each measurement, the coil was first entirely filled with the stationary phase. Then the apparatus was run at a desired revolutionary speed while the mobile phase was pumped through the coil at 120 ml/h with a Chromatronix Cheminert pump (Chromatronix, Sunnyvale, CA, U.S.A.). The effluent from the outlet of the coil was collected into a 25-ml graduated cylinder to measure the volume of the stationary phase eluted from the coil and the total volume of the mobile phase eluted. During the run, the temperature inside the centrifuge was controlled at  $22 \pm 1^\circ\text{C}$  by placing an ice-bag



directly over the top plate of the centrifuge. The run was continued for 10 min or slightly longer so that the effluent volume exceeded the total capacity of the coil. Then, the apparatus was stopped and the coil was emptied by connecting the inlet of the coil to a nitrogen gas line at a pressure of *ca.* 80 p.s.i. The coil was then flushed with several milliliters of methanol miscible with both phases. Finally, the coil was again flushed with several milliliters of the stationary phase to be used in the next experiment. During emptying and flushing of the coil with nitrogen, the apparatus was rotated at a moderate speed of 100–200 rpm in a direction making the coil outlet the head to promote the drainage of the column contents.

For the coils mounted at the center of the coil holder, the measurements were mainly performed in two elution modes as shown in Table I, each at four different revolutional speeds of 200, 300, 400, and 500 rpm using both upper and lower phases as the mobile phase in each solvent system. It has been observed that the coils mounted at 10-cm left from the center of the holder, where the laterally acting centrifugal force field becomes asymmetric, yield different levels of stationary phase retention according to the direction of the planetary motion and handedness of the coil as well as the head-tail elution mode, thus totaling eight combinations of experimental conditions as summarized in Table II. All these combinations were tested with the 25-cm diameter holder at 500 rpm by the use of both right-handed and left-handed coils each mounted at 10 cm left from the center of the holder. In the rest of the cases, the measurements were limited to four combinations with right-handed coils at 500 rpm. Any experimental condition which produced significant degree of retention at 500 rpm was further examined under reduced revolutional speeds of 400, 300 and 200 rpm to obtain phase distribution diagrams described below.

### Phase distribution diagrams

From each experiment, retention of the stationary phase was expressed as a percentage relative to the total column capacity according to the expression,  $100(V_c + V_f - V_s)/V_c$ , where  $V_c$  denotes the total capacity of the coil;  $V_f$ , free space in the flow tubes; and  $V_s$ , the volume of the stationary phase eluted from the coil.

TABLE I  
TWO ELUTION MODES AT CENTRAL COIL POSITION ( $l = 0$  cm)



| Planetary motion                                                                             | Head-tail elution mode (handedness of coil)* | Combined elution modes** | Design in PDD*** |
|----------------------------------------------------------------------------------------------|----------------------------------------------|--------------------------|------------------|
| $P_I$     | Head-to-tail (R)                             | $P_I$ -H                 | ———              |
| $P_{II}$  | Tail-to-head (R)                             | $P_{II}$ -T              | -----            |

\* R = Right-handed.

\*\* H = Head-to-tail; T = tail-to-head.

\*\*\* PDD = Phase distribution diagram.

TABLE II  
EIGHT DIFFERENT ELUTION MODES AT LATERAL COIL POSITION ( $l = -10$  cm)

| Planetary motion                                                                           | Head-tail elution mode | Inward-outward elution mode (handedness of coil*) | Combined elution mode** | Symbols in PDD*** |
|--------------------------------------------------------------------------------------------|------------------------|---------------------------------------------------|-------------------------|-------------------|
| $P_I$     | Head-to-tail           | Inward (R)                                        | $P_I$ -H-I              | ○—○               |
|                                                                                            | Head-to-tail           | Outward (L)                                       | $P_I$ -H-O              | ○- -○             |
|                                                                                            | Tail-to-head           | Inward (L)                                        | $P_I$ -T-I              | ●- -●             |
|                                                                                            | Tail-to-head           | Outward (R)                                       | $P_I$ -T-O              | ●- -●             |
| $P_{II}$  | Head-to-tail           | Inward (L)                                        | $P_{II}$ -H-I           | △ -△              |
|                                                                                            | Head-to-tail           | Outward (R)                                       | $P_{II}$ -H-O           | △—△               |
|                                                                                            | Tail-to-head           | Inward (R)                                        | $P_{II}$ -T-I           | ▲- -▲             |
|                                                                                            | Tail-to-head           | Outward (L)                                       | $P_{II}$ -T-O           | ▲- -▲             |

\* R = right-handed; L = left-handed.

\*\* H = head-to-tail; T = tail-to-head; I = inward; O = outward.

\*\*\* PDD = phase distribution diagram.

Using the retention data thus obtained, the hydrodynamic distribution of the two solvent phases in the coil was summarized in a phase distribution diagram which was constructed by plotting percentage retention of the stationary phase as a function of revolutionary speed for each mobile phase. A group of retention curves produced by different elution modes but otherwise identical experimental conditions can be illustrated in the same diagram. In order to distinguish each elution mode in the phase distribution diagram, a set of symbolic designs was used to draw phase distribution curves as illustrated in Tables I and II.

## RESULTS AND DISCUSSION

A series of experiments was performed with nine two-phase solvent systems to study the distribution of two solvent phases in the coil mounted on a set of holders located at the center of the holder ( $l = 0$  cm) and 10 cm to the left of the center ( $l = -10$  cm). The results obtained revealed the important findings that the degree of stationary phase retention was different at the two locations on the same holder and that in the lateral coil position retention of the stationary phase was significantly affected by the direction of the planetary motion and the head-tail elution modes. Therefore, the results obtained from these two coil locations are described separately.

### Phase distribution diagrams obtained from central coil position ( $l = 0$ cm)

The results of phase retention studies obtained with the central coil position are summarized in Fig. 3, where a set of phase distribution diagrams is arranged according to the format used in the previous studies<sup>2</sup>. In this figure, each column consists of phase distribution diagrams obtained from the solvent system labelled and arranged from left to right in the order of the hydrophobicity of the major organic component. As indicated in the left-hand margin, the top three rows show the retention of the lower phase obtained by elution with the upper phase, and the bottom three rows the

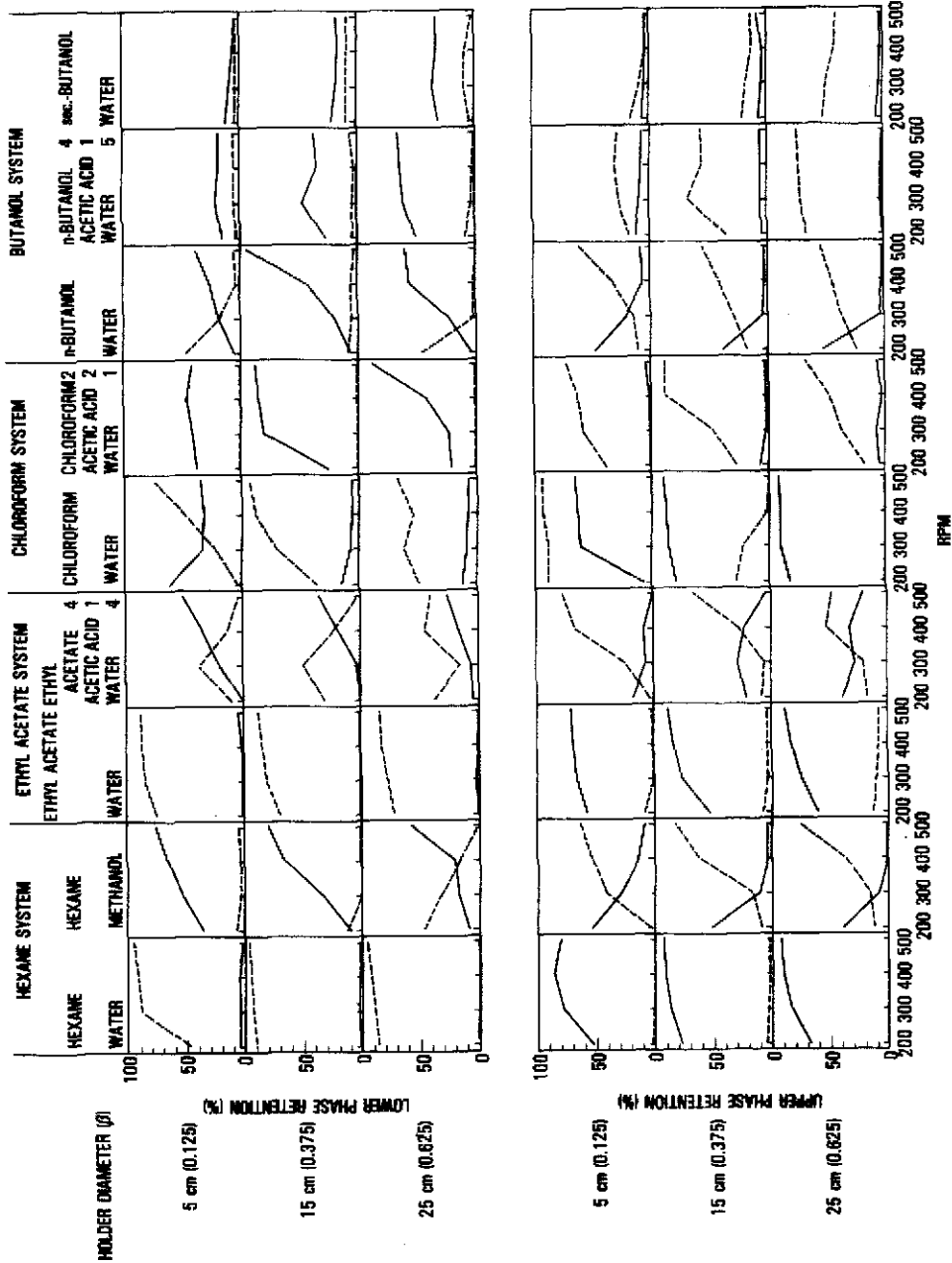


Fig. 3. A set of phase distribution diagrams for nine volatile solvent systems obtained from the central coil position ( $l = 0$  cm). See Table I for designs for phase distribution curves. (—) Head  $\rightarrow$  tail; (---) tail  $\rightarrow$  head.



retention of the upper phase by elution with the lower phase, and within each mobile phase group the first row was obtained with the 5-cm diameter coil or at  $\beta = 0.125$ , the second row with the 15-cm diameter coil or at  $\beta = 0.375$  and the third row with the 25-cm diameter coil or at  $\beta = 0.625$ . As defined previously<sup>1</sup> and shown in Fig. 1,  $\beta$  is the ratio between the radius of rotation (distance from the central axis of the holder to the coil) and the radius of revolution (distance from the central axis of the centrifuge to the axis of the holder). This determines both the magnitude and direction of the centrifugal force field acting on the various locations of the holder. Two retention curves in each diagram were obtained from each elution mode: the solid curve indicates the head-to-tail elution and the broken curve the tail-to-head elution.

Phase distribution diagrams obtained from the central coil position in this study share common features with those from the original X-axis CPC with a 10-cm revolutionary radius and may be similarly divided into three categories according to hydrophobicity or polarity of the solvent system.

Hydrophobic binary solvent systems characterized by high interfacial tension between the two phases, including hexane-water, ethyl acetate-water and chloroform-water, show high retention when the upper phase is eluted from the tail toward the head (broken curves in the upper column) or the lower phase from the head toward the tail (solid curves in the lower column). On the other hand, hydrophilic solvent systems associated with low interfacial tension, such as *n*-butanol-acetic acid-water (4:1:5) and *sec.*-butanol-water, display an opposite hydrodynamic trend, giving better retention by eluting either the upper phase from the head toward the tail (solid curves in the upper column) or the lower phase from the tail toward the head (broken curves in the lower column). The rest of the solvent systems with intermediate degrees of hydrophobicity generally show a hydrodynamic trend similar to that of the hydrophilic solvent systems but mostly yield a much higher retention level. In both hydrophilic and intermediate solvent systems, the retention is sensitively affected by the  $\beta$  values. In the hydrophilic solvent group the retention is substantially improved at greater  $\beta$  values whereas retention of the intermediate solvent systems changes with the  $\beta$  values in various ways. Hexane-methanol is more highly retained at small  $\beta$  values whereas chloroform-acetic acid water (2:2:1) shows the highest retention at the moderate  $\beta$  value of 0.375.

The overall results obtained with the central coil position indicate that, compared with the original X-axis CPC operated at 200–800 rpm, the present system yields a lower retention for intermediate solvent systems but a substantially improved retention of hydrophilic solvent systems at large  $\beta$  values.

#### *Phase distribution diagrams obtained from lateral coil position ( $l = -10$ cm)*

A set of phase distribution diagrams obtained from the coil mounted 10 cm to the left of the center of the holder is illustrated in Fig. 4 with the same format as used in Fig. 3.

As mentioned earlier, the coil mounted at a lateral location is subjected to an asymmetric lateral force field between the upper and lower halves of the rotating holder, thus causing different levels of retention according to the combination of direction of the planetary motion and elution modes of the mobile phase. The possible combinations are summarized in Table II. As defined in the table, planetary motion  $P_I$  is identical with the motion of the disc shown in Fig. 1, and  $P_{II}$  is the reversed motion

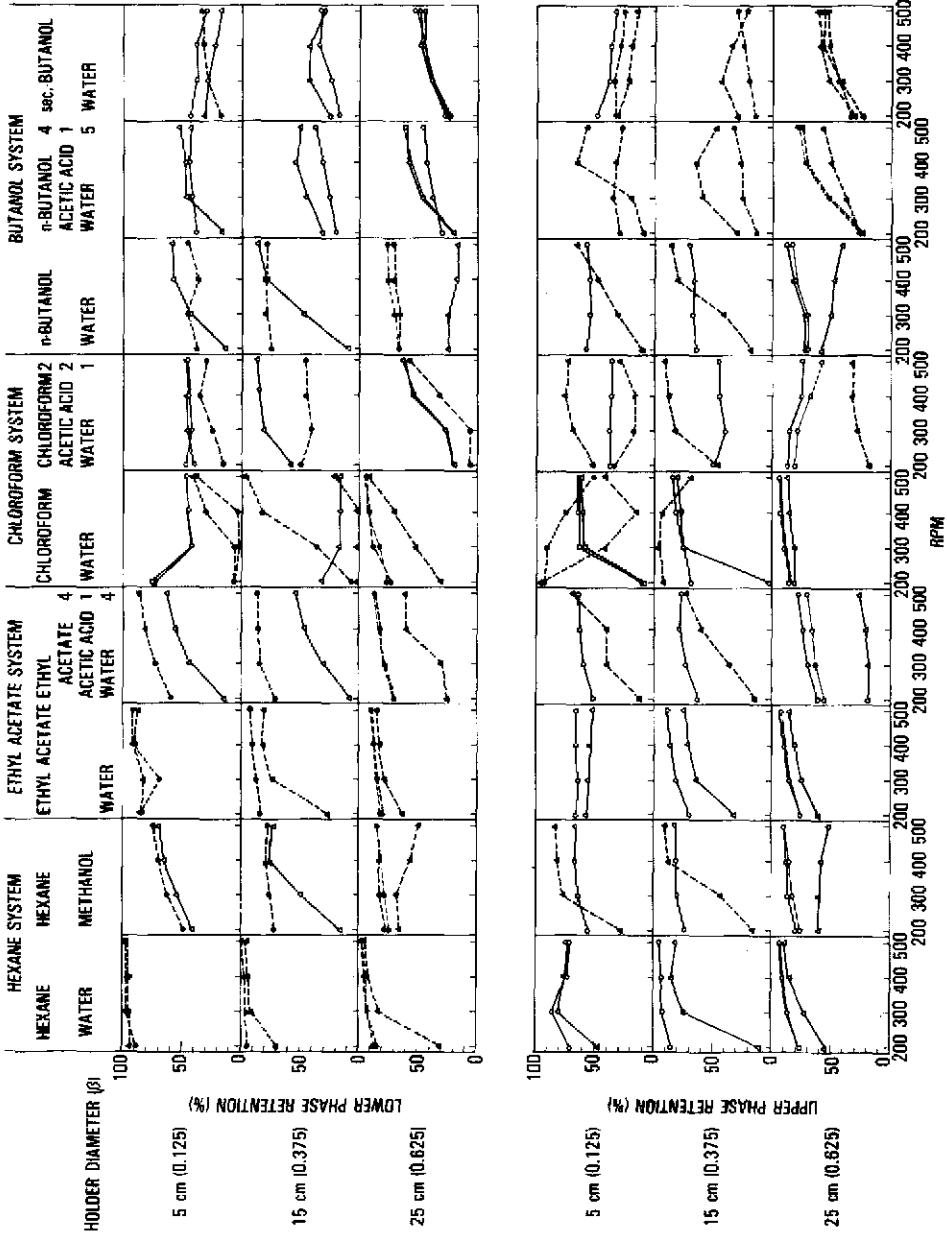


Fig. 4. A set of phase distribution diagrams for nine volatile solvent systems obtained for the lateral coil position ( $l = 0, 10, 20$  cm). See Table II for symbols of phase distribution curves.

resulting in both rotation and revolution of the holder being reversed. In each planetary motion, the mobile phase can be eluted in either the head-to-tail or the tail-to-head mode, thus yielding four different combinations. For each of these four combinations, there is a choice of elution in either the inward or outward direction, which requires the use of both right-handed and left-handed coils. Consequently, a total of eight experimental conditions are possible for each solvent system. Table II shows a set of symbolic designs which were used to distinguish phase distribution curves obtained from different experimental conditions.

All these combinations were first examined with the 25-cm diameter holder ( $\beta = 0.625$ ) at 500 rpm (Table III) and among those the three combinations with the best retention were further tested at various revolutional speeds to draw phase distribution curves as shown in Fig. 4 (bottom row in each mobile phase group). These data clearly indicated that the choice of inward-outward elution modes has little effect on the retention. This is seen by the small difference in the heavy and light lines connecting the same symbols. Therefore, the remainder of the studies on the 15- and 5-cm diameter holders were performed exclusively with the right-handed coils to investigate the effects of the two other parameters, *i.e.*, the planetary motion and the head-tail elution mode. All four combinations possible with the right-handed coils were tested at 500 rpm and two or more combinations which produced significant retention values were further studied at lower rpm to obtain the remaining phase distribution curves (Fig. 4).

The overall results of the retention studies on the lateral coil position revealed a considerable improvement in retention over those obtained with the central coil position for almost all solvent systems. Intermediate solvent systems such as hexane-methanol, ethyl acetate-acetic acid-water (4:1:4) and *n*-butanol-water produced excellent retention for all  $\beta$  values with the proper elution mode. A great improvement in retention was also observed in hydrophilic solvent systems which are extremely useful for separations of polar compounds. The retention of *n*-butanol-acetic acid-water (4:1:5) exceeded the 50% level for all  $\beta$  values while that of *sec.*-butanol-water reached 50% at  $\beta = 0.625$ . Although chloroform-containing solvent systems failed to show substantial improvements in retention, they gave satisfactory retention between  $\beta$  values of 0.375 and 0.625, with the highest retention at  $\beta \approx 0.375$ . The foregoing results clearly indicate that the lateral coil position permits satisfactory retention of the stationary phase in all the solvent systems examined, provided that the proper combination of planetary motion and head-tail elution mode is chosen.

Retention data obtained with the two coil positions on each holder can be more conveniently compared in each mobile phase if expressed in a single diagram as shown in Fig. 5A-C. In each diagram, the abscissa indicates the retention values obtained at the central coil position at 500 rpm and the ordinate, those obtained at the lateral coil position under otherwise identical experimental conditions. Each data point is marked with a specific symbol assigned for the applied experimental condition (planetary motion and head-tail elution mode) as indicated in Table II (see also the caption to Fig. 5). In order to specify the applied solvent systems, these points are individually labelled 1-9, each number corresponding to a particular two-phase solvent system as specified in the figure caption.

A diagonal drawn in each diagram divides the whole area into two equal parts;

TABLE III

RETENTION (%) OF STATIONARY PHASE IN A COIL POSITIONED Laterally ON THE 25-cm DIAMETER HOLDER AT 500 rpm

| Mobile phase  | Solvent system* |            |                 |            |               |             |                          |             |      |
|---------------|-----------------|------------|-----------------|------------|---------------|-------------|--------------------------|-------------|------|
|               | Hexane-water    |            | Hexane-methanol |            | EtOAc-water   |             | EtOAc-AcOH-water (4:1:4) |             |      |
|               | Condition**     | %          | Condition       | %          | Condition     | %           | Condition                | %           |      |
| Upper         | $P_1$ -T-O      | 97.2       | $P_1$ -T-I      | 85.0       | $P_1$ -T-O    | 91.0        | $P_1$ -T-I               | 87.0        |      |
|               | $P_1$ -T-I      | 96.9       | $P_1$ -T-O      | 83.1       | $P_1$ -T-I    | 89.8        | $P_1$ -T-O               | 86.4        |      |
|               | $P_{1r}$ -T-O   | 94.4       | $P_{1r}$ -T-I   | 74.3       | $P_{1r}$ -T-I | 85.9        | $P_{1r}$ -T-I            | 74.6        |      |
|               | $P_{1r}$ -T-I   | 94.4       | $P_{1r}$ -T-O   | 49.2       | $P_{1r}$ -T-O | 85.3        | $P_{1r}$ -T-O            | 61.6        |      |
|               | $P_1$ -H-O      | 1.7        | $P_1$ -H-I      | 27.1       | $P_1$ -H-O    | 2.3         | $P_{1r}$ -H-I            | 20.9        |      |
|               | $P_1$ -H-I      | 1.7        | $P_{1r}$ -H-O   | 20.9       | $P_1$ -H-I    | 1.7         | $P_{1r}$ -H-O            | 18.4        |      |
|               | $P_{1r}$ -H-O   | 1.7        | $P_1$ -H-O      | 6.2        | $P_{1r}$ -H-I | 1.7         | $P_1$ -H-O               | 7.9         |      |
|               | $P_{1r}$ -H-I   | 0.6        | $P_1$ -H-I      | 0.8        | $P_{1r}$ -H-O | 0.6         | $P_1$ -H-I               | 5.1         |      |
|               | Lower           | $P_1$ -H-O | 94.4            | $P_1$ -H-I | 89.8          | $P_1$ -II-I | 93.5                     | $P_1$ -II-I | 78.5 |
|               |                 | $P_1$ -H-I | 93.5            | $P_1$ -H-O | 89.3          | $P_1$ -H-O  | 92.1                     | $P_1$ -H-O  | 70.6 |
| $P_{1r}$ -H-I |                 | 90.1       | $P_{1r}$ -H-O   | 56.5       | $P_{1r}$ -H-O | 87.3        | $P_{1r}$ -H-O            | 45.2        |      |
| $P_{1r}$ -H-O |                 | 89.8       | $P_{1r}$ -H-I   | 51.4       | $P_{1r}$ -H-I | 85.3        | $P_{1r}$ -H-I            | 27.1        |      |
| $P_{1r}$ -T-O |                 | 2.8        | $P_{1r}$ -T-O   | 17.5       | $P_{1r}$ -T-I | 9.3         | $P_{1r}$ -T-O            | 14.7        |      |
| $P_1$ -T-I    |                 | 2.3        | $P_1$ -T-I      | 16.9       | $P_{1r}$ -T-O | 8.5         | $P_{1r}$ -T-I            | 11.0        |      |
| $P_{1r}$ -T-I |                 | 2.0        | $P_{1r}$ -T-I   | 13.3       | $P_1$ -T-O    | 6.8         | $P_1$ -T-O               | 7.9         |      |
| $P_1$ -T-O    |                 | 2.0        | $P_1$ -T-O      | 9.0        | $P_1$ -T-I    | 5.6         | $P_1$ -T-I               | 5.6         |      |

\* EtOAc = ethyl acetate; AcOH = acetic acid;  $\text{CHCl}_3$  = chloroform; BuOH = butanol.

\*\* Elution mode as described in Table II.

the area above the line indicates the improved retention for the lateral position and that below the line lowered retention. The longer the distance of a point from the diagonal, the greater is the effect on retention. The diagram is also divided evenly into four small squares by thin lines, each square having a specific implication: the upper left and lower right squares represent satisfactory retention of over 50% in the lateral coil ( $l = -10$  cm) and in the centered coil ( $l = 0$  cm), respectively, while the upper right square provides satisfactory retention for both coils and the lower left square unsatisfactory retention for either coil. Further, if the upper right square contains two different symbols with the same shading and the same number, satisfactory retention is provided in the coil mounted throughout the width of the holder ( $-10$  cm  $< l < 10$  cm), whereas if the same is observed in the upper left square, satisfactory retention is limited to both left and right lateral positions excluding the central part of the holder ( $l = -10$  cm and 10 cm).

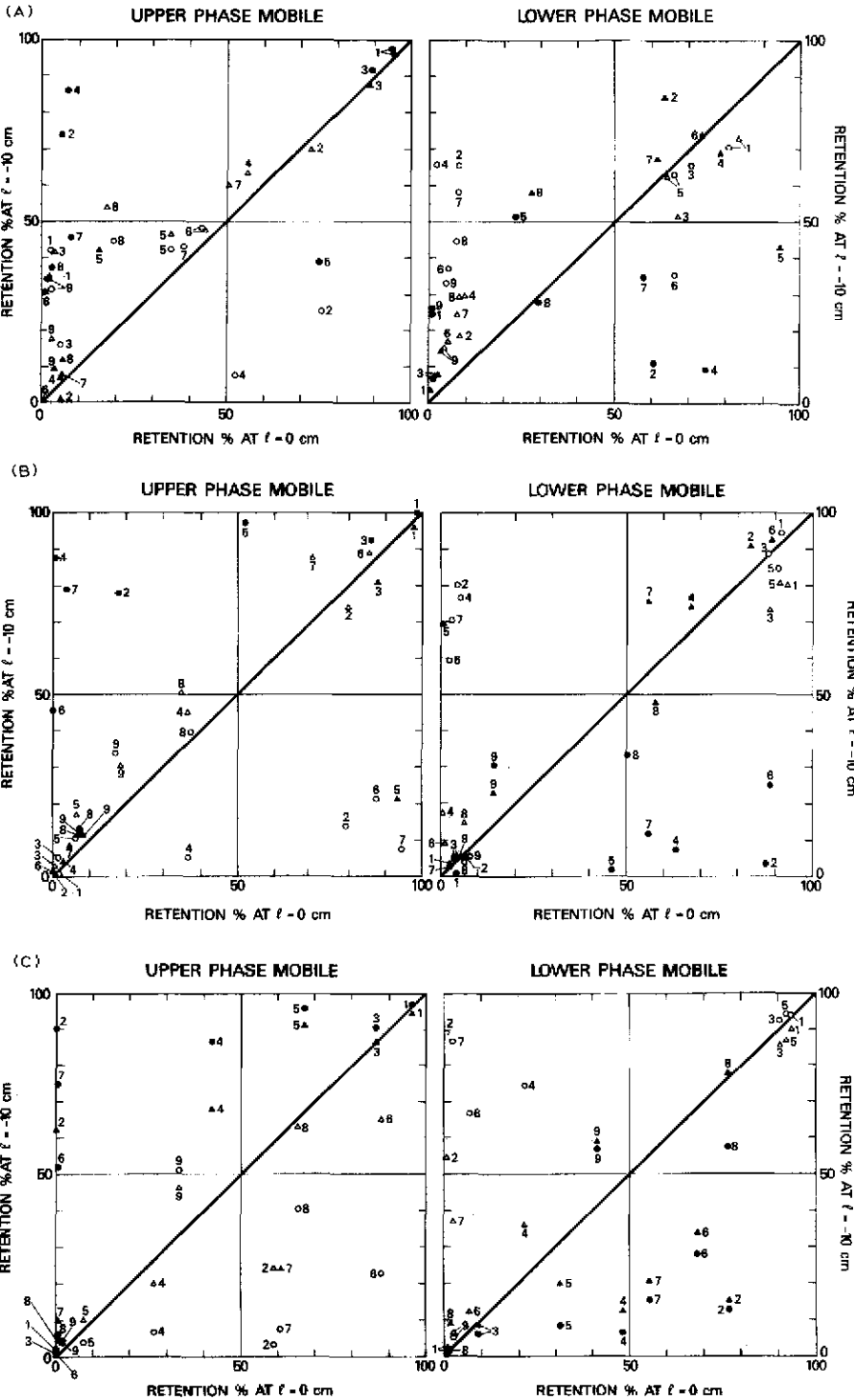
While the above indication for applicability of the coil positions can also be extracted from Figs. 3 and 4 and Table III without much difficulty, these diagrams further furnish invaluable information by disclosing a peculiar hydrodynamic effect associated with the lateral coil position. For example, in Fig. 5B ( $\beta = 0.375$ ) solid circles (tail-to-head elution under planetary motion,  $P_1$ ) and open triangles (head-to-tail elution under planetary motion  $P_{1r}$ ) dominate above the diagonal if the upper phase is mobile (left), whereas open circles (head-to-tail elution under planetary

| <i>CHCl<sub>3</sub>-water</i> |      | <i>CHCl<sub>3</sub>-AcOH-water (2:2:1)</i> |      | <i>n-BuOH-water</i>       |      | <i>n-BuOH-AcOH-water (4:1:5)</i> |      | <i>sec.-BuOH-water</i>    |      |
|-------------------------------|------|--------------------------------------------|------|---------------------------|------|----------------------------------|------|---------------------------|------|
| Condition                     | %    | Condition                                  | %    | Condition                 | %    | Condition                        | %    | Condition                 | %    |
| <i>P<sub>I</sub>-T-I</i>      | 96.0 | <i>P<sub>II</sub>-H-I</i>                  | 65.0 | <i>P<sub>I</sub>-T-I</i>  | 77.4 | <i>P<sub>II</sub>-H-I</i>        | 64.1 | <i>P<sub>I</sub>-H-O</i>  | 52.5 |
| <i>P<sub>I</sub>-T-O</i>      | 95.5 | <i>P<sub>II</sub>-H-O</i>                  | 64.4 | <i>P<sub>I</sub>-T-O</i>  | 71.5 | <i>P<sub>II</sub>-H-O</i>        | 62.1 | <i>P<sub>I</sub>-H-I</i>  | 49.2 |
| <i>P<sub>II</sub>-T-O</i>     | 94.4 | <i>P<sub>I</sub>-T-I</i>                   | 57.3 | <i>P<sub>II</sub>-H-O</i> | 30.2 | <i>P<sub>I</sub> II-O</i>        | 46.9 | <i>P<sub>II</sub>-H-O</i> | 47.5 |
| <i>P<sub>II</sub>-T-I</i>     | 87.6 | <i>P<sub>I</sub>-T-O</i>                   | 46.6 | <i>P<sub>II</sub>-H-I</i> | 17.8 | <i>P<sub>I</sub>-H-I</i>         | 33.7 | <i>P<sub>II</sub>-H-I</i> | 45.8 |
| <i>P<sub>II</sub>-H-O</i>     | 10.2 | <i>P<sub>I</sub>-H-O</i>                   | 24.3 | <i>P<sub>II</sub>-T-I</i> | 10.2 | <i>P<sub>II</sub>-T-I</i>        | 7.6  | <i>P<sub>I</sub>-T-O</i>  | 8.2  |
| <i>P<sub>II</sub>-H-I</i>     | 9.6  | <i>P<sub>I</sub>-H-I</i>                   | 21.5 | <i>P<sub>II</sub>-T-O</i> | 9.0  | <i>P<sub>I</sub>-T-I</i>         | 7.3  | <i>P<sub>II</sub>-T-O</i> | 6.2  |
| <i>P<sub>I</sub>-H-O</i>      | 3.9  | <i>P<sub>I</sub>-T-I</i>                   | 0    | <i>P<sub>I</sub>-H-O</i>  | 8.0  | <i>P<sub>I</sub> T-O</i>         | 4.5  | <i>P<sub>II</sub>-T-I</i> | 0.8  |
| <i>P<sub>I</sub>-H-I</i>      | 3.4  | <i>P<sub>II</sub>-T-O</i>                  | 0    | <i>P<sub>I</sub>-H-I</i>  | 7.3  | <i>P<sub>II</sub>-T-O</i>        | 1.1  | <i>P<sub>I</sub>-T-I</i>  | 0.6  |
| <i>P<sub>I</sub>-H-O</i>      | 94.9 | <i>P<sub>I</sub>-H-I</i>                   | 74.9 | <i>P<sub>I</sub>-H-I</i>  | 88.7 | <i>P<sub>II</sub>-T-O</i>        | 78.5 | <i>P<sub>II</sub>-T-I</i> | 61.6 |
| <i>P<sub>I</sub>-H-I</i>      | 93.8 | <i>P<sub>I</sub>-H-O</i>                   | 58.2 | <i>P<sub>I</sub> H-O</i>  | 84.7 | <i>P<sub>II</sub>-T-I</i>        | 75.7 | <i>P<sub>I</sub>-T-O</i>  | 58.2 |
| <i>P<sub>II</sub>-H-O</i>     | 87.0 | <i>P<sub>II</sub>-T-I</i>                  | 35.0 | <i>P<sub>II</sub>-H-I</i> | 40.7 | <i>P<sub>I</sub>-I-I</i>         | 58.2 | <i>P<sub>II</sub>-T-O</i> | 56.5 |
| <i>P<sub>II</sub>-H-I</i>     | 87.0 | <i>P<sub>II</sub>-T-O</i>                  | 33.1 | <i>P<sub>II</sub>-H-O</i> | 33.3 | <i>P<sub>I</sub>-T-O</i>         | 57.1 | <i>P<sub>I</sub>-T I</i>  | 55.9 |
| <i>P<sub>II</sub>-T-I</i>     | 22.6 | <i>P<sub>I</sub>-T-O</i>                   | 32.2 | <i>P<sub>II</sub>-T-I</i> | 25.4 | <i>P<sub>II</sub>-H-I</i>        | 10.7 | <i>P<sub>II</sub>-H-I</i> | 8.5  |
| <i>P<sub>II</sub>-T-O</i>     | 17.7 | <i>P<sub>I</sub>-T-I</i>                   | 24.3 | <i>P<sub>II</sub>-T-O</i> | 16.9 | <i>P<sub>II</sub>-H-O</i>        | 7.3  | <i>P<sub>I</sub>-H-I</i>  | 6.8  |
| <i>P<sub>I</sub>-T-I</i>      | 10.2 | <i>P<sub>II</sub>-H-I</i>                  | 14.7 | <i>P<sub>I</sub>-T-O</i>  | 16.1 | <i>P<sub>I</sub>-H-I</i>         | 2.0  | <i>P<sub>II</sub>-H-O</i> | 5.1  |
| <i>P<sub>I</sub>-T-O</i>      | 6.8  | <i>P<sub>II</sub>-H-O</i>                  | 10.1 | <i>P<sub>I</sub>-T-I</i>  | 15.3 | <i>P<sub>I</sub>-H-O</i>         | 1.7  | <i>P<sub>I</sub>-H-O</i>  | 3.9  |

motion  $P_I$ ) and solid triangles (tail-to-head elution under planetary motion  $P_{II}$ ) dominate above the diagonal if the lower phase is mobile (right). These findings strongly suggest that the direction of the planetary motion is in some way closely related to the head-tail elution mode to govern the hydrodynamics in the lateral coil position, thus providing an important clue for speculation on the hydrodynamic mechanism associated with the X-axis CPC as discussed below.

#### *Hydrodynamic effect of the lateral coil shift: a hypothesis*

As described earlier, lateral shift or replacement of the coil results in a considerable improvement in retention of the stationary phase in almost all of the solvent systems examined. In order to explain this phenomenon, we must first consider the centrifugal force field generated by the planetary motion of the holder previously analysed<sup>1</sup>. Fig. 6 shows the distribution of the centrifugal force vectors acting on the rotating holder at various  $\beta$  values in both central ( $l = 0$  cm) (right) and lateral ( $l = -10$  cm) (left) coil positions. In each diagram,  $O_b$  is on the central axis of the holder and the axis of the centrifuge is shown as a vertical line tangent to the outermost circle labelled  $\beta = 1.0$  on the left side of each diagram. The centrifugal force acting on various points of the holder is divided into two components, *i.e.*, arrows for the main force vectors acting in the  $X_b-Y_b$  plane and the thick columns for the secondary force vectors acting perpendicularly to the  $X_b-Y_b$  plane, where the ascending columns



indicate the force vectors directed above the plane and the descending columns the force vectors acting below the plane. As clearly shown in these diagrams, the lateral shift of the point along the axis of the holder develops an asymmetric lateral force field (columns) between the upper and the lower halves of the holder, while the main centrifugal force field acting across the axis of the holder remains unaltered.

Both the enhanced retention of the stationary phase in the lateral coil position and the close correlation between the planetary motion and the head-tail elution mode observed in Fig. 5 may be explained on the basis of this asymmetry of the laterally acting force field.

Fig. 7 illustrates coils at the lateral position on the holder undergoing planetary motion  $P_I$  (left) and planetary motion  $P_{II}$  (right). Because rotation and revolution are simultaneously reversed, these two planetary motions produce the identical force field while reversed rotation of the holder causes reversal of the head-tail orientation of the coil. Under the main centrifugal force field directed radially toward the right as indicated by a large arrow, the upper (lighter) phase is driven toward the left and the lower (heavier) phase toward the right in major portions of the coil.

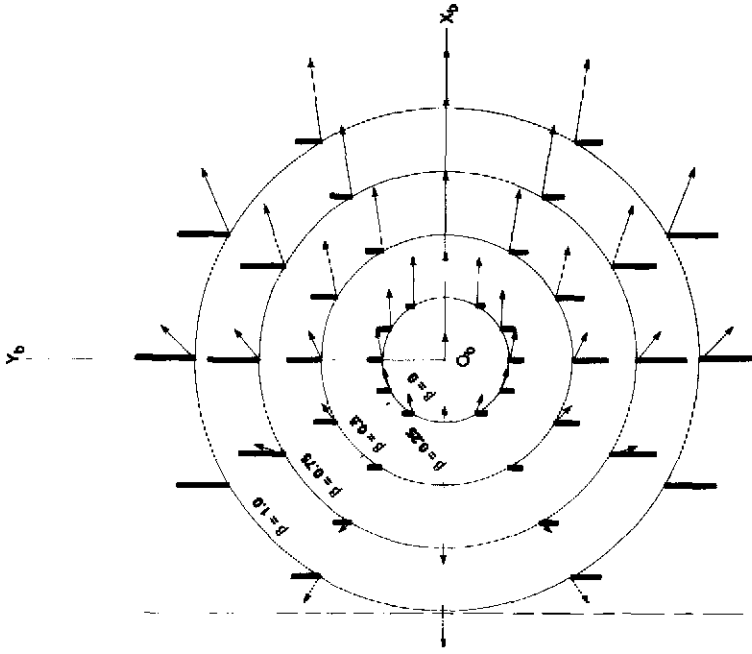
In Fig. 7 (left), planetary motion  $P_I$  determines the coil rotation, hence the head-tail orientation of the coil as indicated by a pair of curved arrows at the top and the bottom of the diagram. Owing to the asymmetric lateral force field between the upper and lower halves of the coil, the countercurrent movement of the two solvent phases is accelerated in the upper portion of the coil owing to suppressed emulsification while the movement is decelerated in the lower portion of the coil owing to enhanced emulsification. Consequently, in this situation the tail-to-head elution of the upper phase (solid circles in Fig. 5B, left) and the head-to-tail elution of the lower phase (open circles in Fig. 5B, right) result in enhanced retention of the stationary phase.

In Fig. 7 (right), planetary motion  $P_{II}$  reverses both the rotation and the head-tail orientation of the coil as illustrated. Owing to the asymmetric lateral force field left unaltered, the countercurrent movement of the two solvent phases is similarly accelerated on the upper portion of the coil and decelerated in the lower portion of the coil. Therefore, in this case the head-to-tail elution of the upper phase (open triangles in Fig. 5B, left) and the tail-to-head elution of the lower phase (solid triangles in Fig. 5B, right) result in enhanced retention of the stationary phase.

In the 25-cm diameter holder ( $\beta = 0.625$ ), the hydrodynamic effects on the lateral coil position are substantially modified, as observed in Fig. 5C, where solid symbols dominate above the diagonal in the left diagram (enhanced tail-to-head movement of the upper phase) and open symbols dominate above the diagonal in the right diagram (enhanced head-to-tail movement of the lower phase). This may be caused by the lateral force field acting on the proximal and distal portions of the coil to alter hydrodynamic trends of the two solvent phases to promote tail-to-head movement of the upper phase and head-to-tail movement of the lower phase, as briefly

Fig. 5. Comparison of retention between the central and lateral coil positions. (A) 5-cm hub diameter; (B) 15-cm hub diameter; (C) 25-cm hub diameter. Symbols:  $\circ$ , planetary motion  $P_I$ , head-to-tail elution mode;  $\bullet$ , planetary motion  $P_I$ , tail-to-head elution mode;  $\Delta$ , planetary motion  $P_{II}$ , head-to-tail elution mode;  $\blacktriangle$ , planetary motion  $P_{II}$ , tail-to-head elution mode. Solvent systems: 1 = hexane-water; 2 = hexane-methanol; 3 = ethyl acetate-water; 4 = ethyl acetate-acetic acid-water (4:1:4); 5 = chloroform-water; 6 = chloroform-acetic acid-water (2:2:1); 7 = *n*-butanol-water; 8 = *n*-butanol-acetic acid-water (4:1:5); 9 = *sec.*-butanol-water.

**FORCE DISTRIBUTION AT CENTRAL COIL POSITION  
( $l = 0$  cm)**



**FORCE DISTRIBUTION AT LATERAL COIL POSITION  
( $l = -10$  cm)**

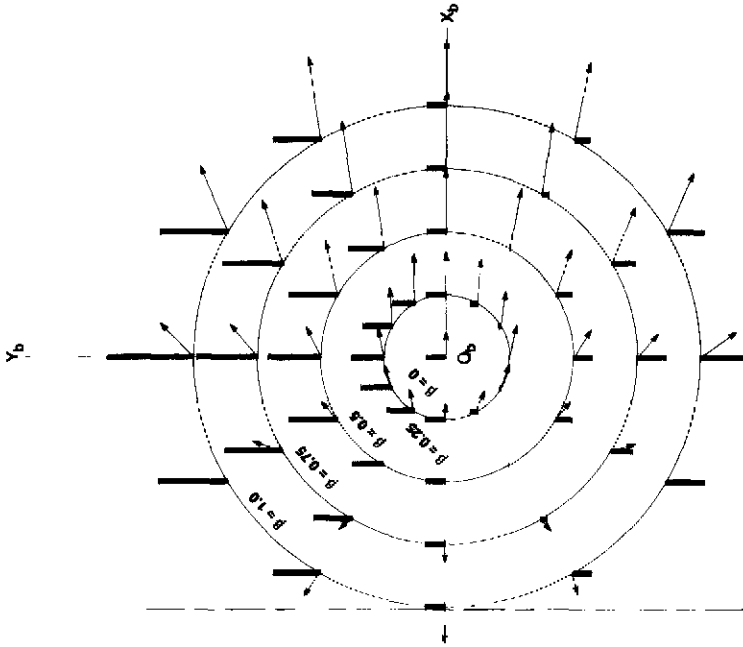


Fig. 6. Force distribution diagrams at two locations of the coil on the holder in the cross-axis synchronous flow-through coil planet centrifuge. Right, central position ( $l = 0$  cm); left, lateral position ( $l = -10$  cm).



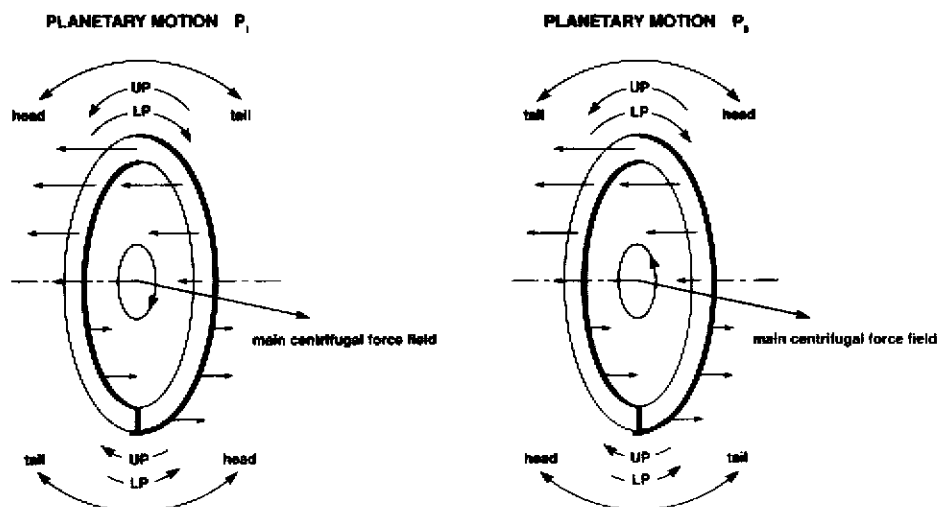


Fig. 7. Hydrodynamic effects of the asymmetric lateral force field formed at the lateral coil position ( $l = -10$  cm). Left, planetary motion  $P_I$ ; right, planetary motion  $P_{II}$ . UP, upper (lighter) phase; LP, lower (heavier) phase.

suggested elsewhere<sup>5</sup>. On a large diameter holder, this effect may overcome that of the asymmetric lateral force field acting on the upper and lower sides of the coil. The latter effects, however, are still evident within each elution mode, *i.e.*, a solid circle always locates above the solid triangle in Fig. 5C (left) and an open triangle above the open circle in Fig. 5C (right) for each solvent system.

#### ACKNOWLEDGEMENT

The authors are deeply indebted to Mr. Jimmie L. Slemp, Division of Research Services, Biomedical Engineering and Instrumental Branch, National Institutes of Health, for fabrication of the apparatus.

#### REFERENCES

- 1 Y. Ito, *Sep. Sci. Technol.*, 22 (1987) 1971.
- 2 Y. Ito, *Sep. Sci. Technol.*, 22 (1987) 1989.
- 3 Y. Ito, J. Sandlin and W. G. Bowers, *J. Chromatogr.*, 244 (1982) 247.
- 4 Y. Ito, *J. Chromatogr.*, 403 (1987) 77.
- 5 Y. Ito, *J. Liq. Chromatogr.*, 11 (1988) 1.